Introduction to Bayesian Statistics - 12

Edoardo Milotti

Università di Trieste and INFN-Sezione di Trieste

The oxygen isotope ratio.

The oxygen isotope ratio is the primary method used to determine past temperatures from ice cores. Because isotopes have a different number of neutrons, they have different mass numbers. Oxygen's most common isotope has a mass number of 16 and is written as ^{16}O. Most of the oxygen in water molecules is composed of 8 protons and 8 neutrons in its nucleus, giving it a mass number (the number of protons and neutrons in an element or isotope) of 16. About one out of every 1,000 oxygen atoms contains 2 additional neutrons and is written as ^{18}O.

Depending on climate, the two types of oxygen (^{16}O and ^{18}O) vary in water. Scientists compare the ratio of the heavy (^{18}O) and light (^{16}O) isotopes in ice cores, sediments, or fossils to reconstruct past climates. They compare this ratio to a standard ratio of oxygen isotopes found in ocean water at a depth of 200 to 500 meters. The ratio of the heavy to light oxygen isotopes is influenced mainly by the processes involved in the water or hydrologic cycle.

Evaporation and condensation are the two processes that most influence the ratio of ^{18}O to ^{16}O in the oceans. Water molecules containing ^{16}O evaporate slightly more readily than water molecules containing ^{18}O. At the same time, water vapor molecules containing the ^{18}O condense more readily.

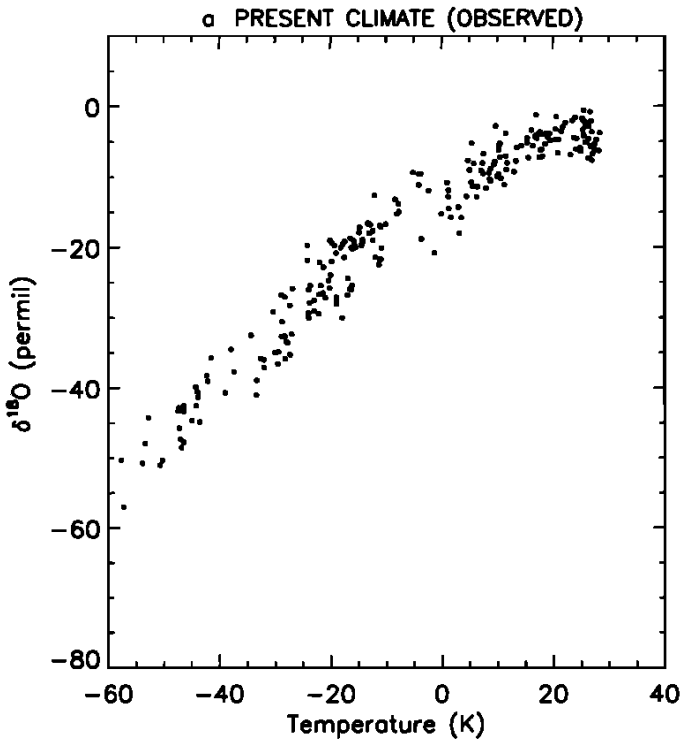

(adapted from https://www.ces.fau.edu/nasa/module-3/how-is-temperature-measured/isotopes.php and https://earthobservatory.nasa.gov/features/Paleoclimatology_OxygenBalance)

The concentration of ^{18}O in precipitation decreases with temperature. This graph shows the difference in ^{18}O concentration in annual precipitation compared to the average annual temperature at each site. The coldest sites, in locations such as Antartica and Greenland, have about 5 percent less ^{18}O than ocean water. (from Jouzel et al., 1994)

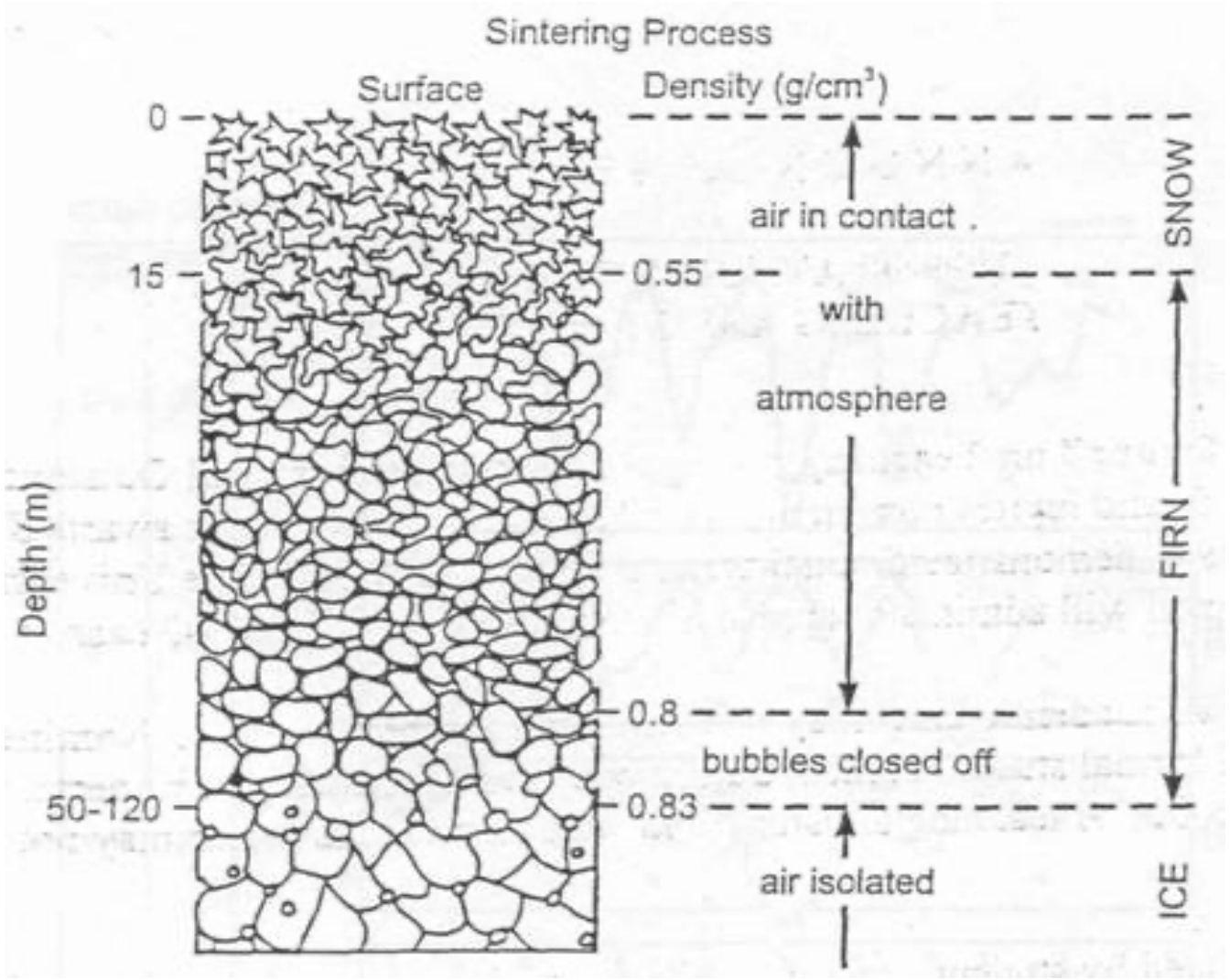
Sintering Process
Surface
Density (g/cm³)
0
15
50-120
Depth (m)
0.55
air in contact
with
atmosphere
0.8
bubbles closed off
0.83
air isolated
SNOW
FIRN
ICE

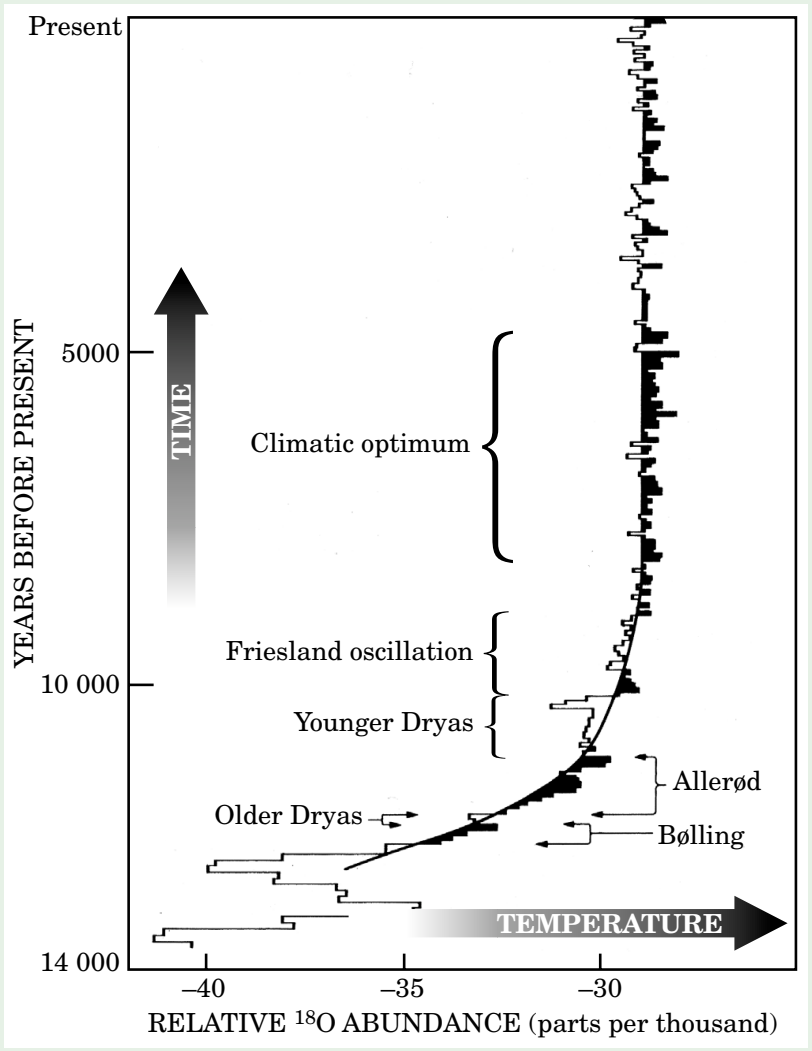

from Weart, Phys. Today 56, 30 (2003)

Figure 3. Cores drilled from the ice at Camp Century, Greenland, and processed on the spot in 1964 (see photo), revealed ancient climate changes in unprecedented detail. The ratio of oxygen-18 to oxygen-16 isotopes in the annual snow layers serves as a thermometer, as shown in the plot: Part per thousand variations to the right indicate warmer temperatures; those to the left, cooler ones. The large rise in temperature started about 14 000 years ago at the end of the last ice age. The plot also shows 1–2°C temperature leaps even within the one-century resolution of the data, but the authors of the 1971 report barely mentioned them in passing. Their concern was the cycles lasting a few centuries or more, which were remarkable enough. Since only a single site was sampled, none of the changes could confidently be called global, and the leaps could have been artifacts due to flow of the deep ice layers. (Photo by David Atwood, courtesy of US Army-ERDC-Cold Regions Research and Engineering Laboratory. Graph adapted from ref. 18.)

08 May 2024 17:49:43

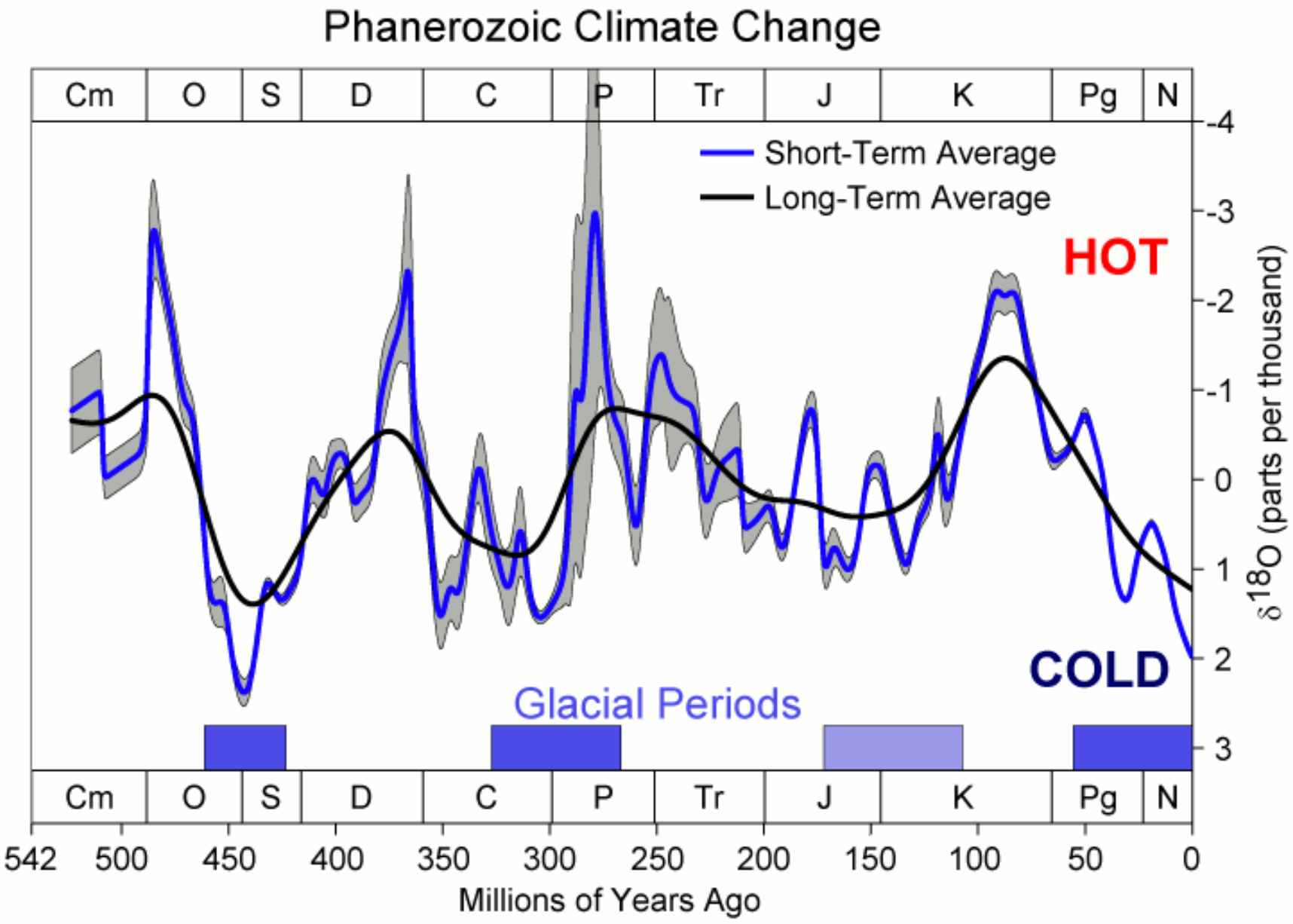
Phanerozoic Climate Change
Cm
O
S
D
C
P
Tr
J
K
Pg
N
Short-Term Average
Long-Term Average
HOT
COLD
Glacial Periods
-4
-3
-2
-1
0
1
2
3
δ18O (parts per thousand)
542
500
450
400
350
300
250
200
150
100
50
0
Millions of Years Ago

Ice core data from lake Vostok in Antarctica

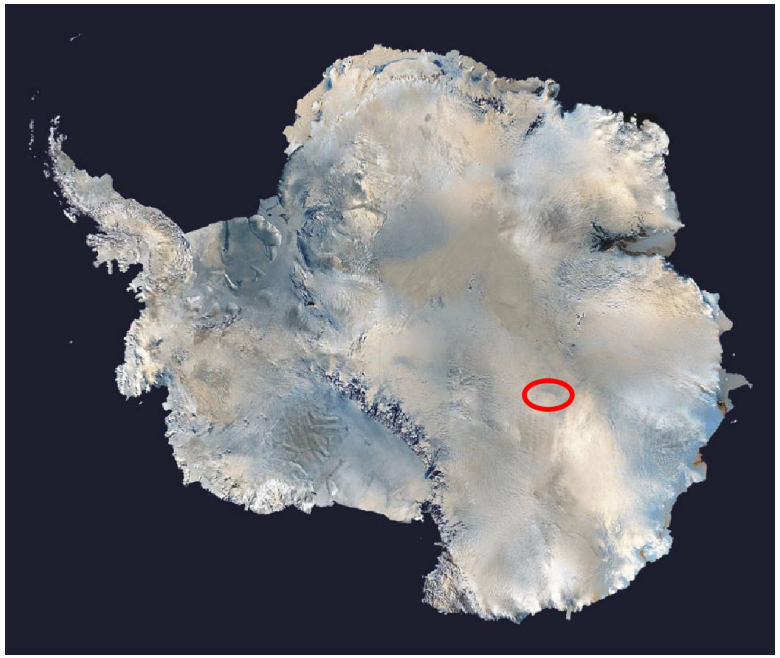

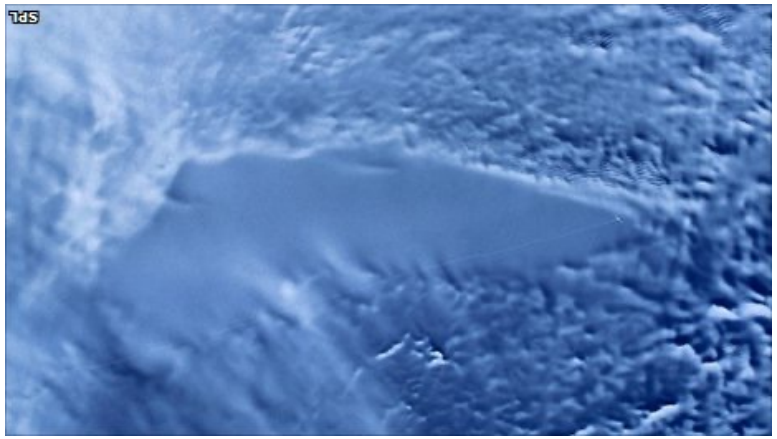

Radar satellite image of lake Vostok

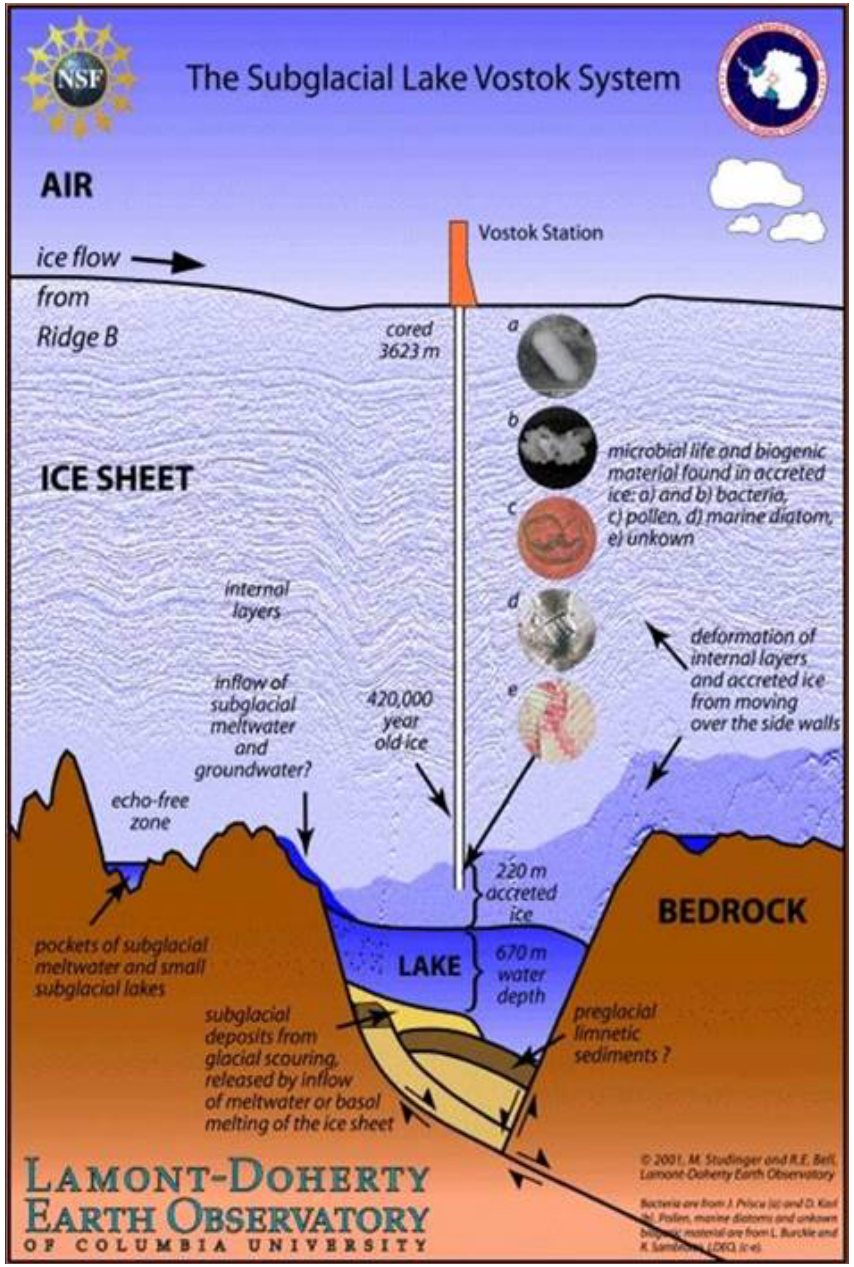

Lake Vostok is the largest of Antarctica's 675 known subglacial lakes.

Lake Vostok is located at the southern Pole of Cold, beneath Russia's Vostok Station under the surface of the central East Antarctic Ice Sheet, which is at 3,488 m above mean sea level.

The surface of this freshwater lake is approximately 4,000 m under the surface of the ice, which places it at approximately 500 m below sea level.

Measuring 250 km long by 50 km wide at its widest point, it covers an area of 12,500 km^2 making it the 16th largest lake by surface area.

With an average depth of 432 m, it has an estimated volume of 5,400 km^3, making it the 6th largest lake by volume.

The lake is divided into two deep basins by a ridge. The liquid water depth over the ridge is about 200 m, compared to roughly 400 m deep in the northern basin and 800 m deep in the southern.

(from Wikipedia, https://en.wikipedia.org/wiki/Lake_Vostok)

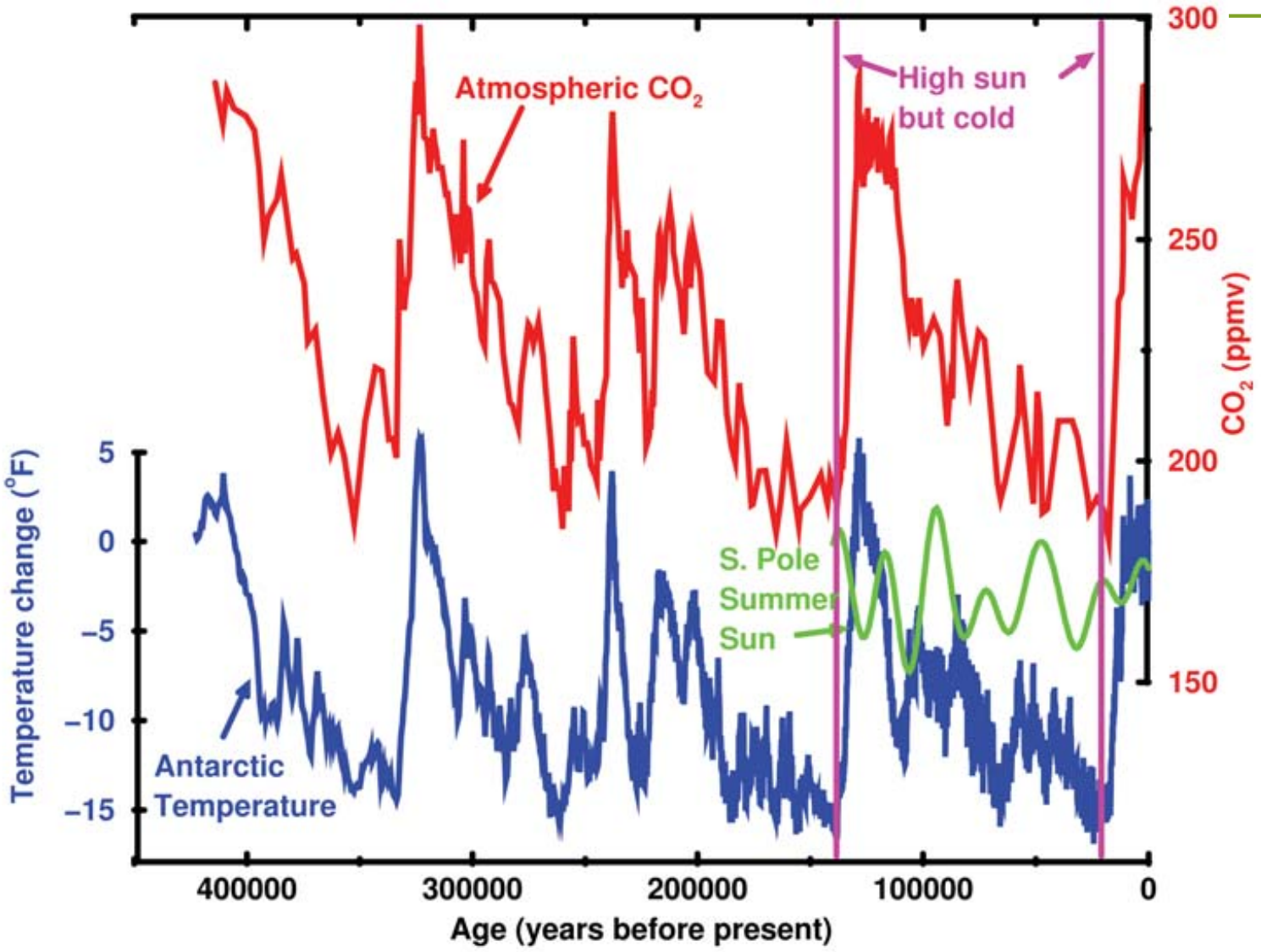

Figure 2. The last 440,000 years of climate in central East Antarctica, from the Vostok ice core. Today is on the right, and 440,000 years ago on the left. The lower curve shows the history of temperature estimated from the isotopic composition of the ice. The large, approximately 100,000-year cycle of ice ages is evident. This basic pattern is also evident in most climate records obtained from anywhere on Earth. Also shown is the variation in local sunshine in Antarctica over the best-dated and more recent part of the record, calculated from knowledge of orbital physics. Peaks in Antarctic sunshine are spaced about 20,000 years apart, and occur when northern sunshine was especially low, including the Antarctic peak in sunshine about 20,000 years ago when Antarctica was especially cold. The only explanation of this behavior that "works" is that the carbon-dioxide concentration of the atmosphere followed northern sunshine, as shown by the upper curve and that, in turn, carbon dioxide was more important for southern temperature than was southern sunshine.

from Alley, 2004

Milankovitch cycles describe the collective effects of changes in the Earth's movements on its climate over thousands of years. The term was coined and named after the Serbian geophysicist and astronomer Milutin Milanković.

In the 1920s, he hypothesized that variations in **eccentricity, axial tilt, and precession** combined to result in cyclical variations in the intra-annual and latitudinal distribution of solar radiation at the Earth's surface, and that this orbital forcing strongly influenced the Earth's climatic patterns.

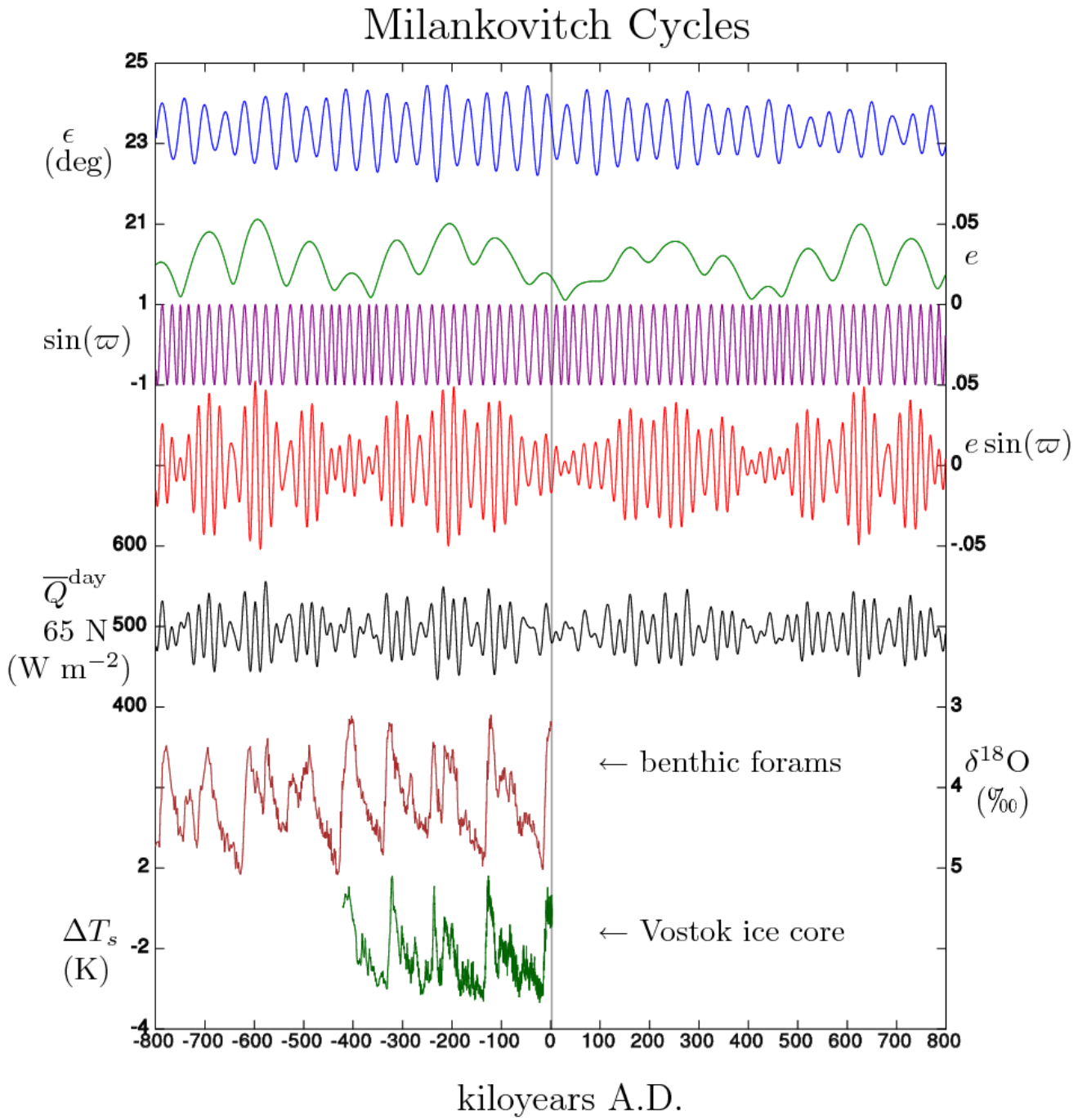

Past and future Milankovitch cycles via VSOP model

- Graphic shows variations in five orbital elements:
  - Axial tilt or obliquity (ε).
  - Eccentricity (*e*).
  - Longitude of perihelion (sin(ϖ)).
  - Precession index (*e* sin(ϖ))
- Precession index and obliquity control insolation at each latitude:
  - Daily-average insolation at top of atmosphere on summer solstice ($\overline{Q}^{\text{day}}$) at 65° N
- Ocean sediment and Antarctic ice strata record ancient sea levels and temperatures:
  - Benthic forams (57 widespread locations)
  - Vostok ice core (Antarctica)
- Vertical gray line shows present (2000 CE)

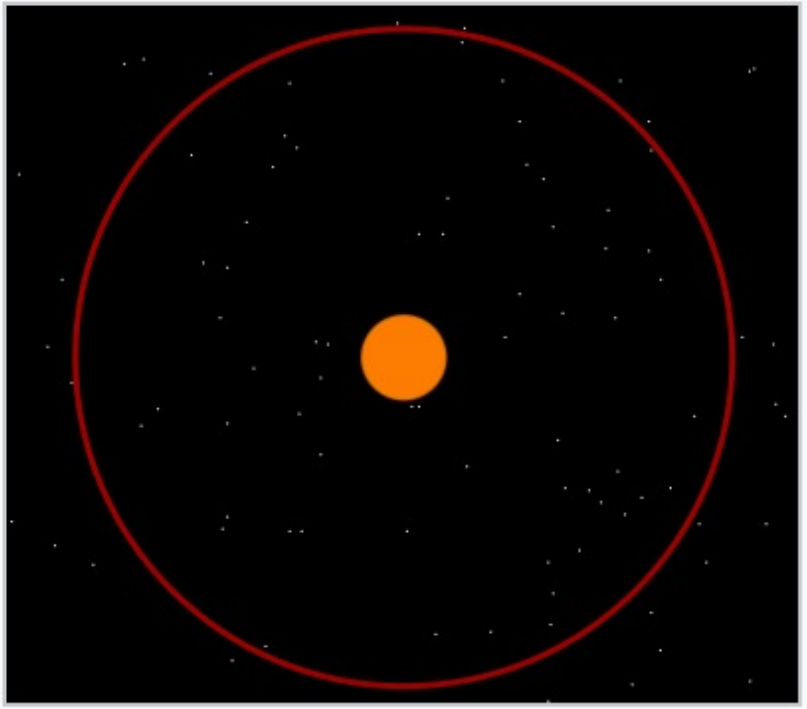

Circular orbit, no eccentricity

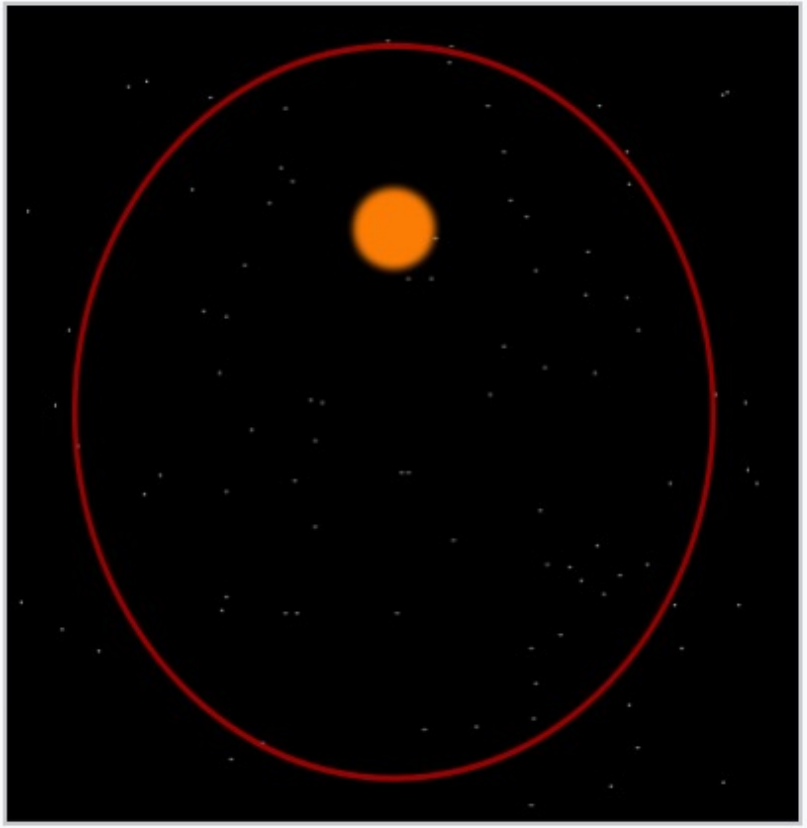

Orbit with 0.5 eccentricity, exaggerated for illustration; Earth's orbit is only slightly eccentric

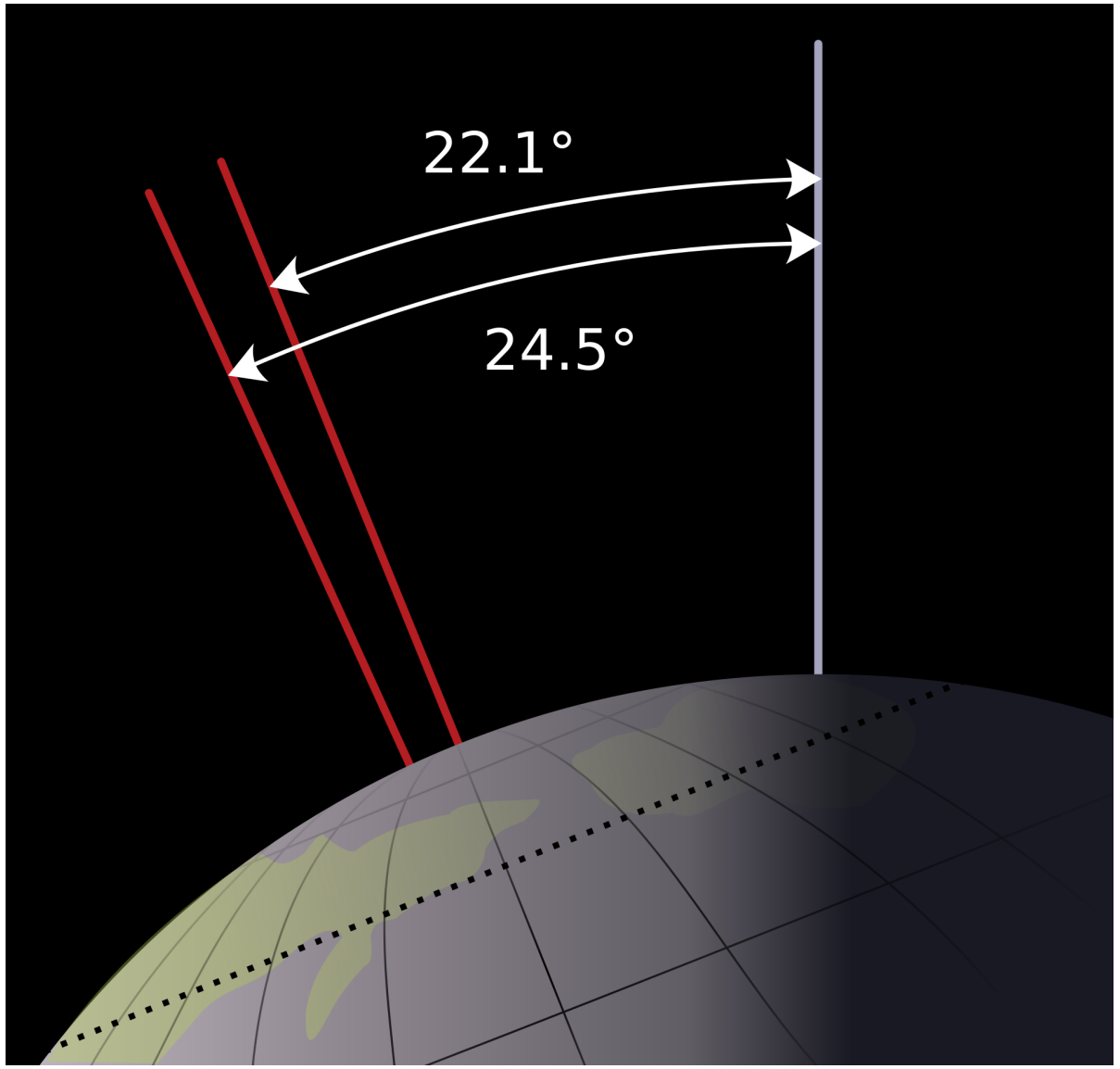

22.1–24.5° range of Earth's obliquity.

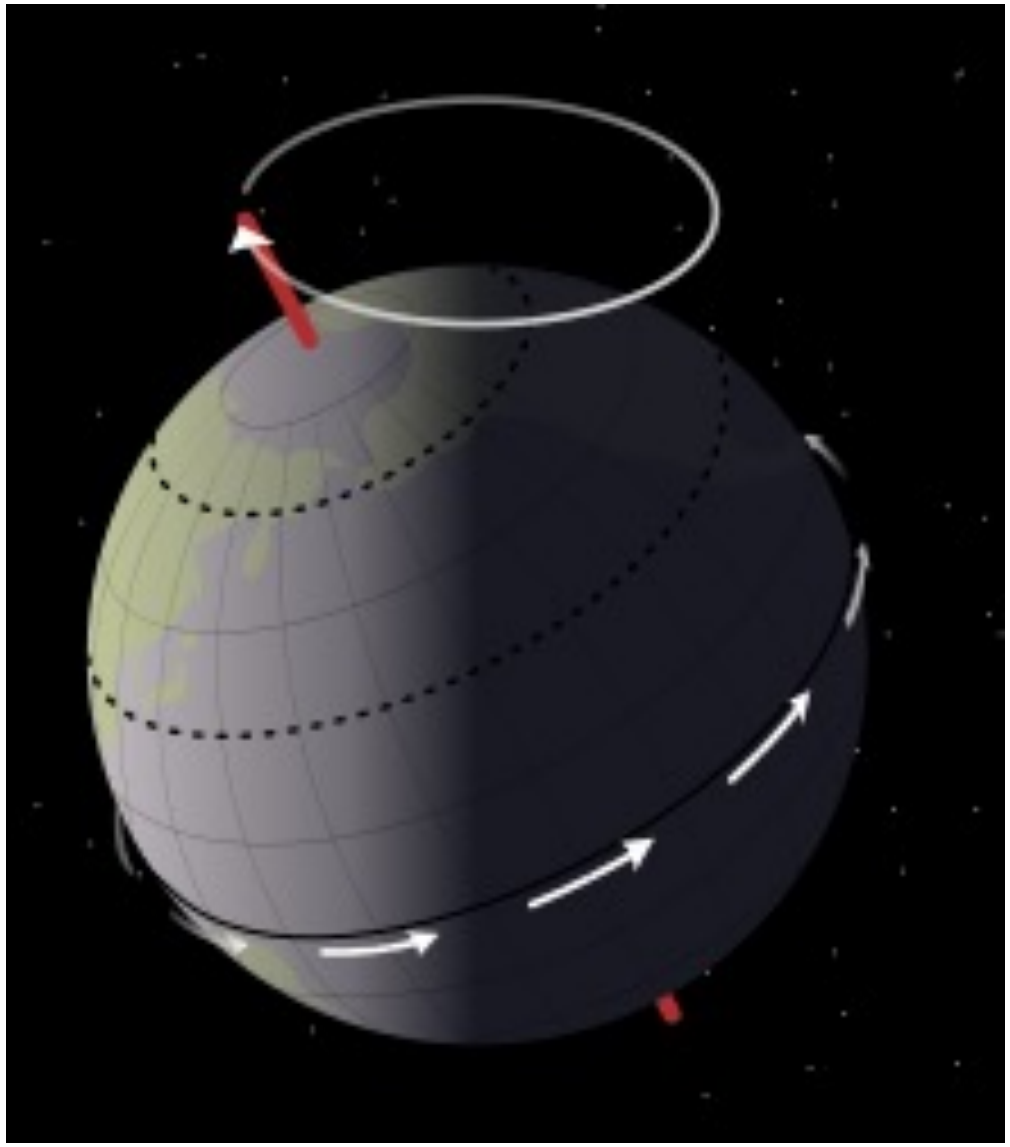

Axial precessional movement.

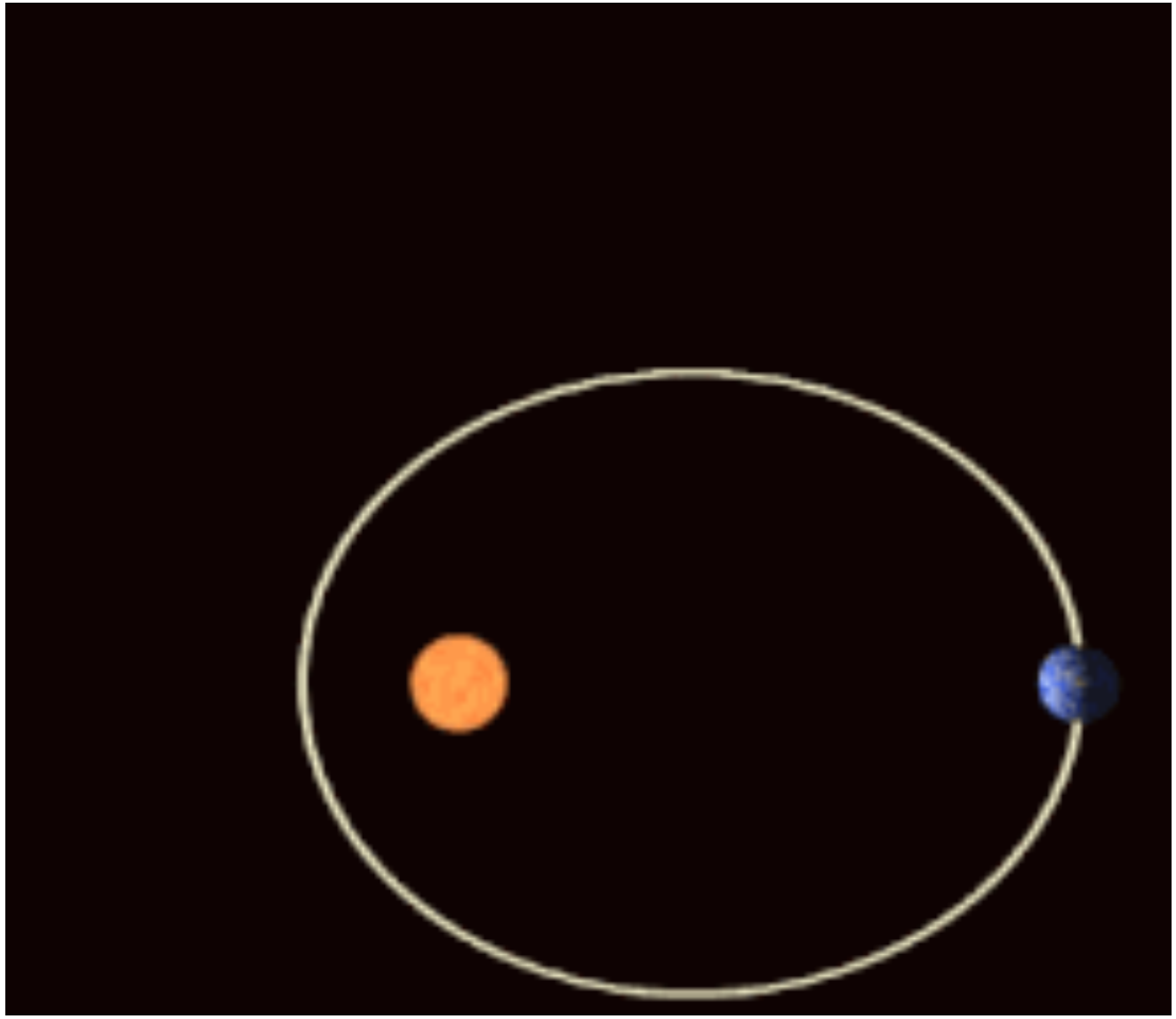

Planets orbiting the Sun follow elliptical (oval) orbits that rotate gradually over time (apsidal precession). The eccentricity of this ellipse, as well as the rate of precession, are exaggerated for visualization

Spectrum Analysis—A Modern Perspective

STEVEN M. KAY, MEMBER, IEEE, AND STANLEY LAWRENCE MARPLE, JR., MEMBER, IEEE

Abstract—A summary of many of the new techniques developed in the last two decades for spectrum analysis of discrete time series is presented in this tutorial. An examination of the underlying time series model assumed by each technique serves as the common basis for understanding the differences among the various spectrum analysis approaches. Techniques discussed include the classical periodogram, classical Blackman-Tukey, autoregressive (maximum entropy), moving average, autoregressive-moving average, maximum likelihood, Prony, and Pisarenko methods. A summary table in the text provides a concise overview for all methods, including key references and appropriate equations for computation of each spectral estimate.

II. Review of Spectral Estimation Techniques
- A. Spectral Density Definitions and Basics
- B. Traditional Methods (Periodogram, Blackman-Tukey)
- C. Modeling and Parameter Identification Approach
- D. Rational Transfer Function Modeling Methods
- E. Autoregressive (AR) PSD Estimation
- F. Moving Average (MA) PSD Estimation
- G. Autoregressive Moving Average (ARMA) PSD Estimation
- H. Pisarenko Harmonic Decomposition (PHD)
- J. Prony Energy Spectral Density Estimation
- K. Prony Spectral Line Estimation
- L. Maximum Likelihood Method (MLM)

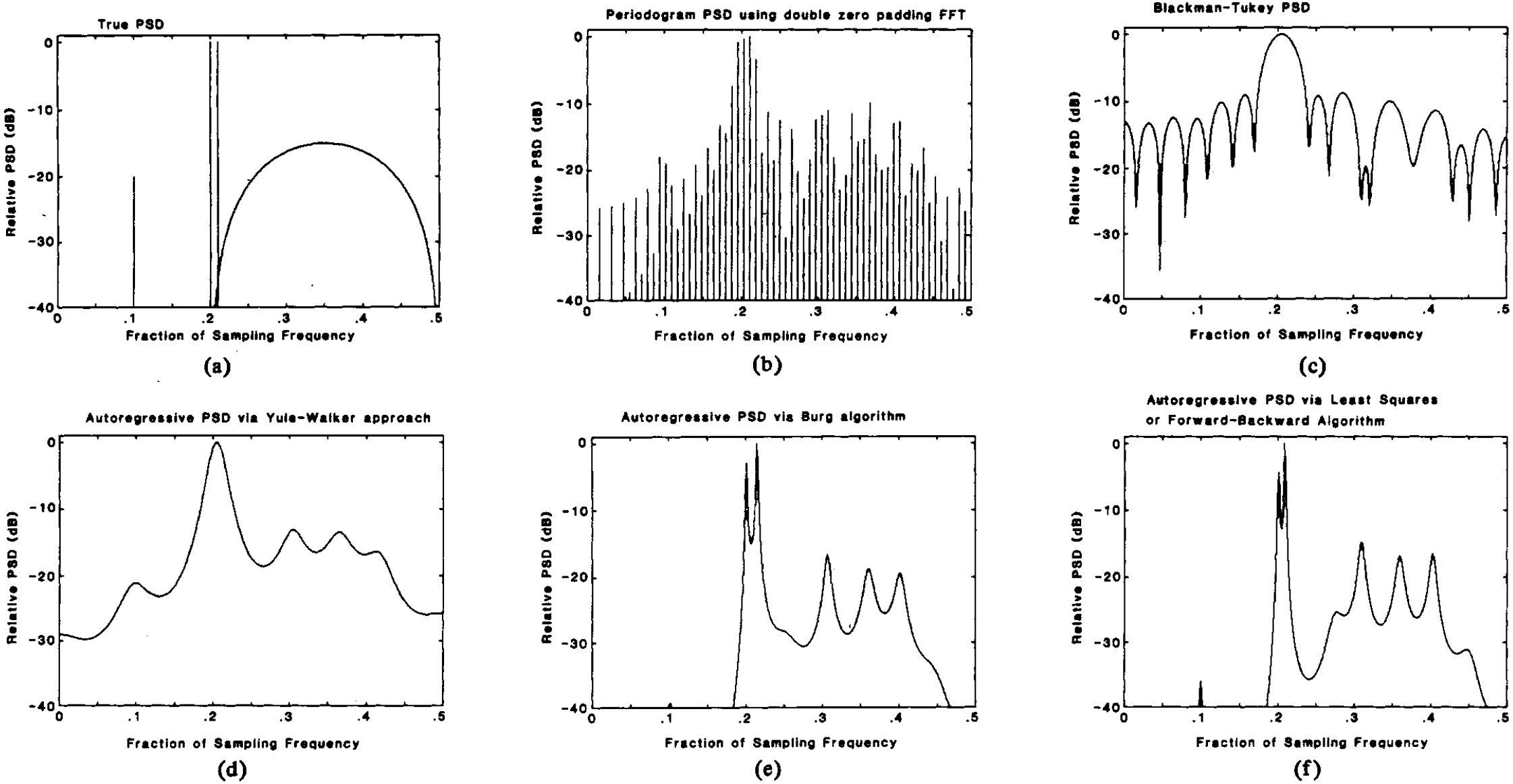

Illustration of various spectra for the same 64-point sample sequence. (from Kay and Marple, 1981)

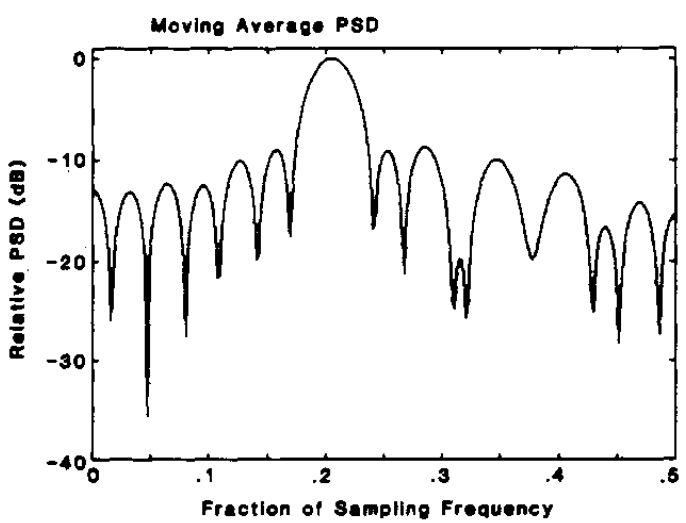

(g)

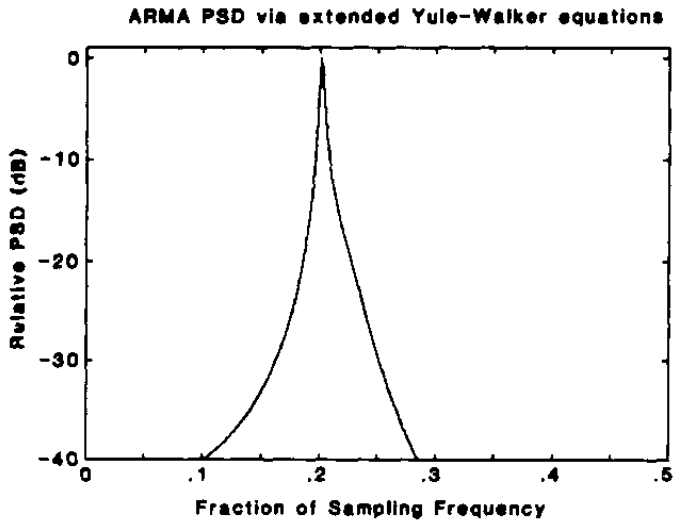

(h)

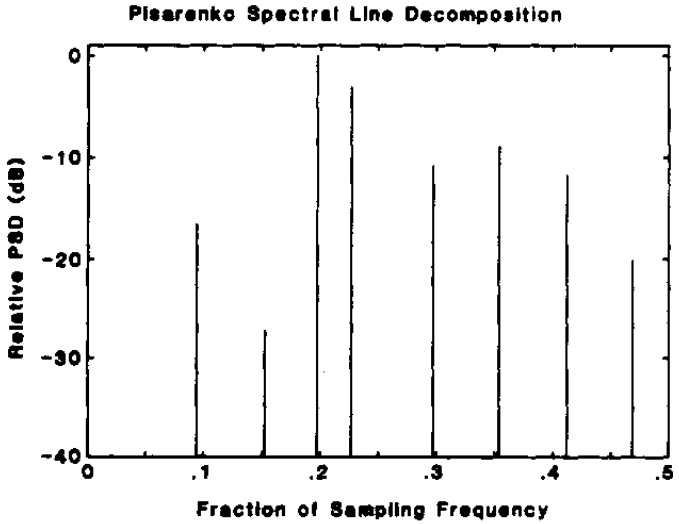

(i)

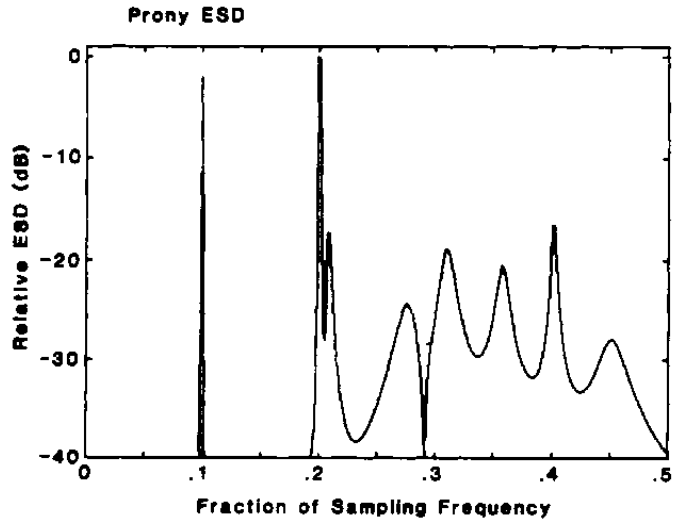

(j)

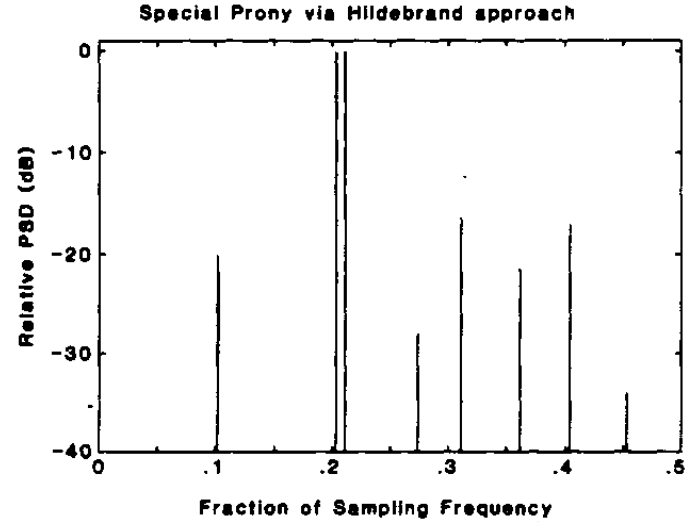

(k)

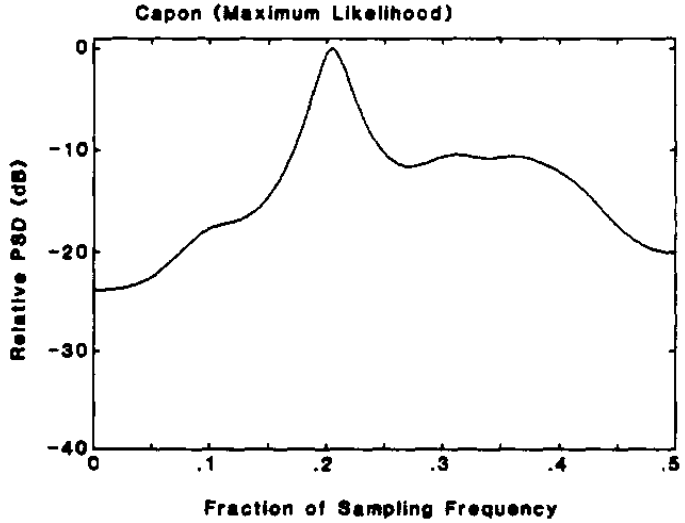

(l)

Illustration of various spectra for the same 64-point sample sequence. (from Kay and Marple, 1981)

Prony's Method (Extended)	95 97 252	C	Fig. 15	AR Coeffs.: $M^2 + NM$ Poly. Rooting: Dependent on Root Algorithm Amp. Coeffs.: M^3 PSD Est.*: MS	Sum of nonharmonically related damped exponentials ARMA with equal MA and AR coefficients and equal orders (p=q)	Must determine order Output linearly proportional to power Requires a polynominal rooting Resolution as good as AR techniques, sometimes better No sidelobes	Uses least squares estimates to obtain exponential parameters First step same as AR least squares estimation
Prony Spectral Line Decomposition	95 226	D	Eqns. (2.161) (2.158) (2.151) (2.153)	Coeffs.: M^3 Rooting: Function of root algorithm used Amp. Coeffs.: M^3	Sum of nonharmonically related sinusoids	Must determine order Output linearly proportional to power Requires a polynominal rooting Resolution as good as AR techqniues, sometimes better No sidelobes	Uses least squares estimation